A&A 411, 381–390 (2003)
DOI: 10.1051/0004-6361:20031399


Astronomy & Astrophysics

# $^{12}$CO(1–0) observation of isolated late-type galaxies⋆,⋆⋆

S. Sauty[1], F. Casoli[1], A. Boselli[2], M. Gerin[1], J. Lequeux[1], J. Braine[3], G. Gavazzi[4], J. Dickey[5], I. Kazès[6], and P. Fouqué[7]

[1] LERMA and FRE 2460 du CNRS, Observatoire de Paris, 61 Av. de l'Observatoire, 75014 Paris, France
[2] Laboratoire d'Astrophysique de Marseille, BP 8, Traverse du Siphon, 13376 Marseille Cedex 12, France
[3] Observatoire de Bordeaux, UMR 5804, CNRS/INSU, BP 89, 33270 Floirac, France
[4] Università degli Studi di Milano-Bicocca, Dipartimento di Fisica, Piazza dell'Ateneo Nuovo 1, 20126 Milano, Italy
[5] Department of Astronomy, University of Minnesota, 116 Church Street, SE, Minneapolis, MN 55455, USA
[6] GEPI, Observatoire de Paris, Section de Meudon, 92195 Meudon Cedex, France
[7] ESO - European Southern Observatory, 3107 Alonso de Cordova, Casilla 19001 Santiago, Chili

Received 3 December 2002 / Accepted 7 September 2003

**Abstract.** We present $^{12}$CO($J$ = 1–0) line observations of 99 galaxies obtained with the SEST 15 m, the Kitt Peak 12 m and the IRAM 30 m telescopes. The target galaxies were selected from the catalogue of isolated galaxies of Karachentseva (1973). These data are thus representative of the CO properties of isolated late-type galaxies. All objects were observed in their central position, those with large angular sizes were mapped. These new measurements are used to estimate the molecular gas mass of the target galaxies. The molecular gas is on average ∼18% of the atomic gas mass.

**Key words.** galaxies: spiral – ISM – intergalactic medium – star formation – radio lines: galaxies

## 1. Introduction

The role of the environment on the evolution of cluster galaxies is still limited by their unknown star formation history. It is still not fully understood whether spirals are affected by a systematic decrease of their star formation activity (SFA) toward the centre of clusters. Such a decrease is expected since their mean HI content, the reservoir and fuel for future star formation, is on average ∼10 times less than in isolated objects of similar morphological type and luminosity (Haynes & Giovanelli 1984).

Since the main gas reservoir in spiral galaxies is HI (Boselli et al. 2001, 2002; Casoli et al. 1998), and because the transformation of atomic gas into molecular clouds is a necessary step before the star formation takes place (in molecular clouds), it is expected that a similar average deficiency may be encountered as well for the molecular gas of spiral galaxies near the core of rich clusters. Early studies of the CO properties of Virgo (Kenney & Young 1989) and Coma (Casoli et al. 1991) galaxies have shown that cluster spirals have, on average, a normal molecular gas content. As pointed out by Boselli (1994) and Boselli et al. (1997, 2002), all these studies were however limited by strong observational biases induced by the use of different criteria (FIR vs. optical) in the selection of cluster and isolated galaxies.

To get rid of these biases, we constructed two reference samples of optically selected isolated galaxies. The first one, presented in Boselli et al. (1997), includes all isolated late-type galaxies extracted from the Zwicky catalogue brighter than $m_{\rm pg} \leq 15.4$ in the Great Wall. Because of its distance (∼90 Mpc) this sample is however limited to bright ($M_{\rm B} \leq -19.4$) galaxies. In order to include lower luminosity ($M_{\rm B} \leq -17.3$) objects we constructed a second reference sample by selecting ∼100 galaxies from the catalogue of isolated galaxies of Karachentseva (1973).

A complete analysis aimed at studying the molecular gas properties of late-type galaxies based on the present set of data joint to other data available in the literature was carried out by Casoli et al. (1998). In synthesis: the gaseous phase of the interstellar medium of late-type galaxies is dominated by the atomic gas, confirming our previous results obtained on a smaller sample (Boselli et al. 1997). This result is here confirmed using a more appropriate luminosity dependent CO to $H_2$ conversion factor.

This paper is devoted to the presentation of the CO observations: because of its uniqueness (composed of strictly isolated, optically-selected late-type galaxies spanning the whole range

*Send offprint requests to*: A. Boselli,
e-mail: Alessandro.Boselli@oamp.fr

⋆ Tables 1 and 2 are also available in electronic form at the CDS via anonymous ftp to cdsarc.u-strasbg.fr (130.79.128.5) or via http://cdsweb.u-strasbg.fr/cgi-bin/qcat?J/A+A/411/381

⋆⋆ Based on observations made with the 12-m National Radio Astronomical Observatory, Kitt Peak, Arizona, with the Swedish-ESO Submillimetre telescope SEST, La Silla, Chile, with the IRAM 30 m radiotelescope, Pico Veleta, Granada, Spain.

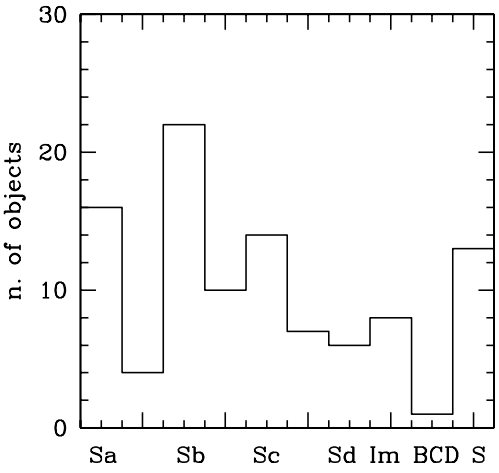


**Fig. 1.** The Hubble type distribution of the observed sample.

in morphological type and luminosity), this sample forms an ideal reference for any statistical study. Joint with the sample of Boselli et al. (1997), it is the unique sample with CO data including strictly isolated galaxies. The unpretentious aim of this paper is to give axcess to the community to these data, whose disponibility might be useful to other astronomers in future studies.

## 2. The sample

The sample analysed in this work has been extracted from the catalogue of isolated galaxies of Karachentseva (1973). A galaxy of diameter $a$ is considered isolated if it is not the potential neighbor of any galaxy of diameter $a_1$ with $1/4a \leq a_1 \leq 4a$, within $20a_1$. The limits and quality of this criterion are extensively discussed in Haynes & Giovanelli (1984). Among the 1051 galaxies of the Karachensteva catalogue, the observed sample has been defined according to the following selection criteria:

- morphological type $\geq$ Sa, to limit the CO observations to gas rich galaxies;
- angular diameter $0.6' \leq a \leq 3.8'$, to exclude both the extended sources, whose mapping would be too time consuming, and the compact sources, where the beam dilution would make the observations unefficient;
- total $B$ magnitude $\leq$15.25;
- with an heliocentric velocity $V_{\rm hel} \leq 14\,000$ km s$^{-1}$.

Four hundred and sixty six galaxies out of 1051 included in the Karachentseva catalogue match these criteria. Of these we serendipitously extracted a subsample of 94 objects. Five objects not matching these criteria were also observed. The observed sample is thus not complete. It includes galaxies spanning the whole range in morphological type (see Fig. 1) and luminosity, from giant spirals to dwarf irregulars ($-21.2 \leq M_{\rm B} \leq -17.3$), although dwarfs are undersampled.

The target galaxies are listed in Table 1 (also available in electronic form at the CDS), arranged as follows:

- Column 1: KIG designation (Karachentseva 1973).
- Column 2: alternative name, from NED.
- Columns 3 and 4: 2000 celestial coordinates with a few arcsec accuracy, from NED.
- Column 5: morphological type, from NED.
- Column 6: isolation class code, from Karachentseva (1973): 0 stands for isolated galaxies, 1 for marginally isolated and 2 for members of a group or cluster.
- Column 7: heliocentric velocity, in km s$^{-1}$, from NED.
- Column 8: total $B$ magnitude as given by NED.
- Columns 9 and 10: galaxy major and minor optical blue diameters, in arcmin, as given by NED.
- Column 11: logarithm of the HI mass, from LEDA[1], determined using the relation: $M(HI) = 2.36 \times 10^5\ D^2\ S\,HI$, where $D$ is the distance of the galaxy (determined from the redshift assuming $H_0 = 75$ km s$^{-1}$ Mpc$^{-1}$) and $S\,HI$ is the HI flux in Jy km s$^{-1}$.
- Column 12: width of the HI line (in km s$^{-1}$), from LEDA, measured at 50% of the maximum intensity, when available, or at 20%.
- Column 13: telescope used: S = SEST, I = IRAM, KP = Kitt Peak.

## 3. The observations

The observations were carried out during 4 observing runs at the SEST 15 m (November 1993–November 1996), one run at the NRAO Kitt Peak[2] 12 m (December 1994) done in remote from the Observatoire de Paris and one run at the IRAM 30 m telescope (June 1996).

At 115 GHz [$^{12}$CO(1–0)], the telescope half-power beam widths (*HPBW*) are 43 arcsec, 55 arcsec and 22 arcsec respectively.

The SEST observations were carried out during fairly good weather conditions. The pointing accuracy was checked every 4 hours by broad band continuum observations of bright continuum sources, with an average error of 4 arcsec rms. We used a Schottky receiver in single sideband mode with typical system temperatures $T_{\rm sys}$ of ~500–600 K (in the $T_{\rm A}^*$ scale). We used a 6 Hz dual beam-switching procedure, with two symmetric reference positions offset by 12 arcmin in azimuth. The backend was an acousto-optical spectrometer of 1440 channels of width 1.4 MHz. Each 12-min scan began with a chopper wheel calibration on a load at ambient temperature and on a cold load.

The Kitt Peak observations were carried out in relatively good weather conditions, with typical zenith opacities of 0.30−0.45. The pointing accuracy was checked every night by broad band continuum observations of Saturn and/or 3C273, with an average error of 7 arcsec rms. We used a dual-polarization SIS mixer, with a receiver temperature for each polarization of about $T_{\rm sys}$ = 260–400 K (in $T_{\rm R}^*$ scale) at the elevation of the sources. We used a dual beam-switching procedure, with two symmetric reference positions offset by 4′ in azimuth. The backend was a 256 channel filter bank spectrometer with

[1] Lyon Extragalactic DAtabase, `http://leda.univ-lyon1.fr/`

[2] The Kitt Peak 12-m telescope was operated by Associated Universities, Inc., under cooperative agreement with the National Science Foundation.

**Table 1.** The target galaxies.

| KIG | Name | RA(2000) h m s | Dec(2000) ° ′ arcsec | Type | Agg | Vel km s$^{-1}$ | Mag | $a$ ′ | $b$ ′ | $M$(HI) $M_\odot$ | $\Delta V_{HI}$ km s$^{-1}$ | Tel |
|---|---|---|---|---|---|---|---|---|---|---|---|---|
| (1) | (2) | (3) | (4) | (5) | (6) | (7) | (8) | (9) | (10) | (11) | (12) | (13) |
| 1 | UGC 5 | 00 03 05.6 | –01 54 49 | SABbc | 0 | 7271 | 13.97 | 1.8 | 0.9 | 10.07 | 458 | S |
| 4 | NGC 7817 | 00 03 58.7 | +20 45 03 | SAbc: s | 0 | 2309 | 12.56 | 3.5 | 0.9 | 9.55 | 398 | KP |
| 6 | NGC 9 | 00 08 54.7 | +23 49 04 | Sb: pec | 2 | 4528 | 14.35 | 1.3 | 0.7 | 9.41 | 163 | KP |
| 11 | UGC 139 | 00 14 31.8 | –00 44 15 | SAB(s)c | 0 | 3963 | 14.49 | 2.1 | 1.0 | 9.93 | 290 | S |
| 22 | IC 1551 | 00 27 35.4 | +08 52 38 | Sc | 0 | 13040 | 14.30 | 2.5 | 1.2 | 9.59 | 146 | S |
| 33 | NGC 237 | 00 43 27.8 | –00 07 30 | SAB(rs) | 0 | 4175 | 13.70 | 1.6 | 0.9 | 9.82 | 296 | S |
| 45 | UGC 685 | 01 07 22.4 | +16 41 02 | Im/BCD | 0 | 157 | 14.23 | 1.2 | 0.9 | 7.14 | 71 | KP |
| 53 | NGC 575 | 01 30 46.7 | +21 26 25 | SB(rs)c | 0 | 3128 | 13.45 | 1.7 | 1.6 | 9.43 | 141 | KP |
| 56 | NGC 622 | 01 36 00.1 | +00 39 49 | SB(rs)b | 0 | 5161 | 13.71 | 1.8 | 1.3 | 9.79 | 372 | S |
| 59 | UGC 1167 | 01 38 20.8 | +07 32 02 | SA(rs)c | 0 | 4303 | 14.00 | 2.7 | 2.1 | 9.86 | 215 | S |
| 68 | NGC 718 | 01 53 13.3 | +04 11 44 | SAB(s)a | 0 | 1733 | 12.59 | 2.3 | 2.0 | 7.38 | 177 | S |
| 72 | UGC 1395 | 01 55 22.0 | +06 36 43 | SA(rs)b | 0 | 5208 | 14.18 | 1.3 | 1.0 | 9.50 | 255 | S |
| 87 | UGC 1587 | 02 05 37.3 | +06 46 19 | Sa | 0 | 5658 | 14.60 | 1.0 | 0.4 | 9.84 | 368 | S |
| 94 | UGC 1706 | 02 13 33.9 | +25 51 20 | Scd: | 0 | 4794 | 14.73 | 1.0 | 0.4 | 9.42 | 275 | KP |
| 115 | IC 1825 | 02 38 55.5 | +09 05 49 | Scd: | 0 | 5125 | 14.55 | 1.2 | 0.8 | 10.08 | 293 | S |
| 123 | IC 302 | 03 12 51.3 | +04 42 25 | SB(rs)b | 0 | 5904 | 13.59 | 1.9 | 1.5 | 10.44 | 249 | S |
| 139 | NGC 1507 | 04 04 27.2 | –02 11 18 | SB(s)m | 0 | 863 | 12.89 | 3.6 | 0.9 | 9.09 | 167 | S |
| 153 | NGC 1544 | 05 02 36.1 | +86 13 20 | S0 | 0 | 3937 | 14.16 | 1.3 | 0.9 | – | – | I |
| 155 | IC 391 | 04 57 21.3 | +78 11 26 | SA(s)c | 0 | 1556 | 13.00 | 1.1 | 1.1 | 9.14 | 145 | KP |
| 166 | UGC 3420 | 06 16 01.4 | +75 56 11 | Sb | 0 | 5106 | 14.10 | 2.6 | 0.8 | 10.26 | 475 | I |
| 176 | UGC 3581 | 06 59 02.8 | +80 00 13 | SAB(rs) | 0 | 4955 | 13.74 | 1.3 | 1.1 | 9.81 | 260 | KP |
| 180 | NGC 2344 | 07 12 28.6 | +47 10 00 | SA(rs)c | 0 | 974 | 12.81 | 1.7 | 1.7 | 8.91 | 147 | KP |
| 191 | UGC 3863 | 07 28 54.1 | +49 08 13 | (R')SBa | 0 | 5918 | 14.01 | 1.2 | 0.6 | 9.55 | 460 | KP |
| 278 | UGC 4531 | 08 41 53.0 | +32 52 03 | Sb | 0 | 7728 | 14.56 | 1.1 | 0.4 | 9.81 | 466 | KP |
| 279 | NGC 2644 | 08 41 31.8 | +04 58 49 | S? | 0 | 1939 | 13.31 | 2.1 | 0.8 | 9.07 | 201 | S |
| 291 | UGC 4684 | 08 56 40.7 | +00 22 30 | SA(rs)d | 0 | 2522 | 14.00 | 1.4 | 1.1 | 9.42 | 157 | I |
| 298 | NGC 2746 | 09 05 59.4 | +35 22 38 | SB(rs)a | 0 | 7065 | 14.00 | 1.6 | 1.5 | 9.89 | 255 | KP |
| 300 | UGC 4781 | 09 06 34.4 | +06 18 13 | Scd: | 0 | 1443 | 14.32 | 1.9 | 0.6 | 9.15 | 143 | I |
| 303 | NGC 2765 | 09 07 36.7 | +03 23 34 | S0 | 2 | 4064 | 13.08 | 2.1 | 1.1 | – | – | S |
| 339 | UGC 5055 | 09 30 11.7 | +55 51 09 | (R')SB | 2 | 7541 | 14.20 | 1.5 | 1.3 | 10.27 | 222 | KP |
| 343 | NGC 2900 | 09 30 15.1 | +04 08 39 | SBcd: | 0 | 5346 | 13.70 | 1.7 | 1.4 | 9.94 | 122 | S |
| 359 | NGC 2960 | 09 40 36.4 | +03 34 37 | Sa? | 0 | 4932 | 13.29 | 1.8 | 1.2 | 9.29 | 435 | S |
| 363 | NGC 2977 | 09 43 46.7 | +74 51 35 | Sb: | 0 | 3044 | 13.30 | 1.8 | 0.8 | 9.08 | 339 | KP |
| 383 | NGC 3049 | 09 54 49.6 | +09 16 17 | SB(rs)a | 0 | 1494 | 13.04 | 2.2 | 1.4 | 9.11 | 200 | S |
| 401 | IC 594 | 10 08 32.0 | –00 40 01 | SB(r)bc | 0 | 6426 | 14.01 | 1.0 | 0.5 | 9.68 | 417 | S |
| 443 | NGC 3376 | 10 47 26.5 | +06 02 53 | S0 | 0 | 5830 | 14.80 | 0.8 | 0.4 | – | – | S |
| 444 | IC 651 | 10 50 58.4 | –02 09 01 | SB(s)m | 0 | 4469 | 13.43 | 0.8 | 0.8 | 9.65 | 192 | S |
| 464 | NGC 3526 | 11 06 56.8 | +07 10 28 | SAc pec | 0 | 1420 | 13.86 | 1.9 | 0.4 | 8.89 | 197 | S |
| 489 | UGC 6568 | 11 35 36.9 | +00 07 40 | SB(s)m | 0 | 5955 | 14.70 | 0.8 | 0.4 | 9.39 | 206 | I |
| 491 | UGC 6608 | 11 38 33.3 | –01 11 04 | SAB(r)a | 0 | 6189 | 14.75 | 1.2 | 0.8 | – | – | S |
| 492 | IC 716 | 11 39 03.3 | –00 12 22 | Sbc pec | 0 | 5429 | 14.80 | 1.6 | 0.3 | 9.81 | 460 | S |
| 499 | UGC 6769 | 11 47 43.7 | +01 49 34 | SB(r)b: | 0 | 8537 | 14.65 | 1.2 | 0.5 | 10.21 | 470 | I |
| 500 | UGC 6771 | 11 48 00.2 | +04 29 18 | (R')SAB | 0 | 5964 | 13.60 | 1.7 | 1.6 | 9.43 | 287 | S |
| 502 | UGC 6780 | 11 48 50.4 | –02 01 57 | SAB(s)d | 0 | 1729 | 15.25 | 3.2 | 1.0 | 9.63 | 223 | S |
| 509 | UGC 6879 | 11 54 25.0 | –02 19 08 | SAB(r)d | 0 | 2383 | 14.08 | 1.7 | 0.6 | 9.08 | 246 | S |
| 512 | UGC 6903 | 11 55 36.9 | +01 14 14 | SB(s)cd | 0 | 1892 | 13.00 | 2.6 | 2.3 | 9.53 | 180 | I |
| 527 | NGC 4348 | 12 23 53.9 | –03 26 35 | SAbc: s | 0 | 2005 | 13.01 | 3.2 | 0.7 | 9.37 | 381 | S |
| 540 | UGC 7798 | 12 38 03.3 | –02 15 50 | IBm: | 0 | 2568 | 14.33 | 0.9 | 0.5 | 9.03 | 206 | S |
| 545 | NGC 4617 | 12 41 06.1 | +50 23 32 | Sb | 0 | 4655 | 14.01 | 3.0 | 0.5 | 10.15 | 458 | KP |
| 547 | NGC 4635 | 12 42 39.1 | +19 56 40 | SAB(s)d | 0 | 960 | 13.20 | 2.0 | 1.4 | 8.48 | 166 | KP |
| 604 | NGC 5377 | 13 56 16.6 | +47 14 08 | (R)SB(s) | 0 | 1793 | 12.24 | 3.7 | 2.1 | 9.16 | 375 | I |
| 605 | NGC 5375 | 13 56 56.0 | +29 09 52 | SB(r)ab | 2 | 2386 | 12.40 | 3.2 | 2.8 | 9.49 | 285 | KP |
| 626 | NGC 5584 | 14 22 23.6 | –00 23 09 | SAB(rs) | 0 | 1635 | 12.63 | 3.4 | 2.5 | 9.50 | 196 | S |
| 638 | NGC 5690 | 14 37 41.0 | +02 17 28 | Sc? sp | 0 | 1753 | 12.50 | 3.4 | 1.0 | 9.58 | 294 | S |

**Table 1.** continued.

| KIG | Name | RA(2000) | Dec(2000) | Type | Agg | Vel | Mag | $a$ | $b$ | $M$(HI) | $\Delta V_{HI}$ | Tel |
|---|---|---|---|---|---|---|---|---|---|---|---|---|
| | | h m s | $^o$ $'$ arcsec | | | km s$^{-1}$ | | $'$ | $'$ | $M\odot$ | km s$^{-1}$ | |
| (1) | (2) | (3) | (4) | (5) | (6) | (7) | (8) | (9) | (10) | (11) | (12) | (13) |
| 652 | NGC 5768 | 14 52 08.1 | –02 31 48 | SA(rs)c | 0 | 1962 | 13.65 | 1.9 | 1.4 | 9.38 | 184 | S,KP |
| 653 | NGC 5772 | 14 51 38.9 | +40 35 57 | SA(r)b: | 1 | 4900 | 13.64 | 2.1 | 1.3 | 9.74 | 501 | KP |
| 669 | NGC 5913 | 15 20 55.4 | –02 34 41 | SB(r)a | 0 | 2004 | 13.87 | 1.6 | 0.7 | 8.69 | 345 | I |
| 695 | CGCG 78-047 | 15 40 53.4 | +09 45 00 | Sa | 0 | 10459 | 14.60 | 0.8 | 0.6 | – | – | S |
| 712 | NGC 6012 | 15 54 13.9 | +14 36 04 | (R)SB(r) | 0 | 1854 | 12.69 | 2.1 | 1.5 | 9.51 | 164 | KP |
| 772 | IC 1231 | 16 46 59.0 | +58 25 23 | Scd: | 0 | 2937 | 13.59 | 2.2 | 1.0 | 9.39 | 381 | KP |
| 785 | UGC 10685 | 17 04 50.9 | +12 55 28 | Sb | 0 | 9642 | 14.50 | 1.8 | 0.6 | 10.25 | 434 | KP |
| 786 | UGC 10699 | 17 06 19.1 | +10 22 31 | Sb | 0 | 6275 | 14.70 | 0.6 | 0.5 | 9.36 | 235 | S |
| 791 | UGC 10743 | 17 11 30.7 | +07 59 40 | Sa? | 0 | 2569 | 14.74 | 1.1 | 0.4 | 9.03 | 213 | S |
| 800 | NGC 6347 | 17 19 54.7 | +16 39 39 | SBb | 2 | 6143 | 14.47 | 1.2 | 0.7 | 9.73 | 370 | S |
| 808 | UGC 10862 | 17 28 08.9 | +07 25 20 | SB(rs)c | 0 | 1691 | 13.40 | 2.8 | 2.5 | 9.32 | 133 | S |
| 812 | NGC 6389 | 17 32 39.8 | +16 24 06 | Sbc | 0 | 3119 | 12.82 | 2.8 | 1.9 | 10.18 | 393 | KP |
| 840 | UGC 11058 | 17 56 55.0 | +32 38 12 | SB(s)b | 0 | 4757 | 13.29 | 1.5 | 1.1 | 9.65 | 278 | KP |
| 850 | NGC 6643 | 18 19 46.6 | +74 34 10 | SA(rs)c | 2 | 1484 | 11.73 | 3.8 | 1.9 | 9.52 | 323 | KP |
| 851 | NGC 6654 | 18 24 07.6 | +73 10 59 | (R')SB | 2 | 1821 | 13.00 | 2.6 | 2.1 | – | – | KP |
| 862 | NGC 6711 | 18 49 00.9 | +47 39 29 | SBbc: | 0 | 4671 | 13.70 | 1.3 | 1.3 | 9.39 | 187 | KP |
| 879 | UGC 11575 | 20 30 07.6 | +03 03 05 | SB(s)d | 0 | 3980 | 14.56 | 1.4 | 0.5 | 9.53 | 305 | S |
| 886 | NGC 6954 | 20 44 03.2 | +03 12 34 | SA0+? | 0 | 4067 | 14.10 | 1.0 | 0.6 | – | – | S |
| 889 | NGC 6969 | 20 48 27.6 | +07 44 23 | Sa | 0 | 4660 | 14.89 | 1.1 | 0.3 | 8.75 | 429 | S |
| 890 | UGC 11635 | 20 43 29.7 | +80 09 22 | Sbc | 0 | 4804 | 13.80 | 2.9 | 1.2 | 10.13 | 485 | KP |
| 897 | NGC 7025 | 21 07 47.3 | +16 20 08 | Sa | 0 | 4968 | 13.71 | 1.9 | 1.3 | 9.47 | 594 | KP |
| 906 | UGC 11723 | 21 20 17.5 | –01 41 03 | Sb | 0 | 4899 | 14.70 | 1.9 | 0.3 | 9.82 | 435 | S,KP |
| 910 | IC 5104 | 21 21 29.3 | +21 14 30 | SBab? | 0 | 4958 | 14.27 | 1.6 | 0.4 | 9.83 | 423 | KP |
| 911 | NGC 7056 | 21 22 07.5 | +18 39 57 | SBb | 0 | 5376 | 13.75 | 1.0 | 0.9 | 9.36 | 233 | S |
| 930 | IC 1401 | 21 46 59.5 | +01 42 45 | SAB(r)b | 0 | 4721 | 14.41 | 1.8 | 0.7 | 9.94 | 364 | S |
| 935 | NGC 7156 | 21 54 33.7 | +02 56 34 | SAB(rs) | 0 | 3985 | 13.11 | 1.6 | 1.4 | 9.57 | 100 | S |
| 940 | UGC 11871 | 22 00 41.4 | +10 33 09 | Sb | 0 | 7978 | 14.48 | 1.1 | 0.7 | 9.68 | 253 | S |
| 949 | UGC 11921 | 22 09 15.4 | +14 21 38 | IBm | 0 | 1678 | 14.35 | 1.7 | 0.7 | 9.04 | 144 | S |
| 976 | NGC 7328 | 22 37 29.2 | +10 31 54 | Sab | 0 | 2825 | 13.98 | 2.0 | 0.7 | 9.70 | 314 | KP |
| 984 | NGC 7367 | 22 44 34.6 | +03 38 44 | Sab: | 0 | 7235 | 14.67 | 1.5 | 0.4 | 9.74 | 570 | KP |
| 985 | UGC 12178 | 22 45 08.5 | +06 25 48 | SAB(s)d | 0 | 1931 | 13.60 | 3.0 | 1.6 | 9.69 | 221 | S |
| 1001 | NGC 7428 | 22 57 19.5 | –01 02 56 | (R)SAB | 0 | 3078 | 13.40 | 2.4 | 1.3 | 9.70 | 316 | S |
| 1003 | UGC 12304 | 23 01 08.4 | +05 39 14 | Sc | 0 | 3470 | 14.72 | 1.7 | 0.2 | 9.13 | 270 | S |
| 1006 | UGC 12372 | 23 07 00.8 | +35 46 39 | Sm | 0 | 5480 | 14.52 | 0.8 | 0.6 | 9.74 | 268 | KP |
| 1009 | NGC 7514 | 23 12 25.8 | +34 52 53 | Sa | 1 | 4843 | 13.54 | 1.4 | 0.9 | 9.41 | 317 | KP |
| 1013 | UGC 12474 | 23 16 43.3 | +33 59 44 | Sa | 2 | 5117 | 14.24 | 1.2 | 0.4 | 9.12 | 357 | KP |
| 1019 | NGC 7664 | 23 26 39.7 | +25 04 49 | Sc: | 0 | 3474 | 13.42 | 1.4 | 0.8 | 10.16 | 329 | KP |
| 1023 | UGC 12646 | 23 31 39.0 | +25 56 44 | SB(r)b | 1 | 8034 | 13.99 | 1.9 | 1.5 | 9.95 | 178 | KP |
| 1027 | UGC 12688 | 23 35 26.2 | +07 19 20 | Sm | 0 | 5229 | 14.27 | 1.7 | 0.4 | 10.00 | 320 | S |
| 1028 | NGC 7712 | 23 35 51.6 | +23 37 07 | E | 0 | 3053 | 13.74 | 0.9 | 0.8 | 9.35 | 179 | KP |
| 1036 | IC 1508 | 23 45 55.0 | +12 03 43 | Sdm: | 0 | 4263 | 13.87 | 2.0 | 0.5 | 10.00 | 321 | KP |
| 1038 | UGC 12776 | 23 46 12.2 | +33 22 12 | SB(rs)b | 1 | 4937 | 13.70 | 2.5 | 2.1 | 10.24 | 247 | KP |
| 1039 | IC 5355 | 23 47 15.4 | +32 46 59 | SBcd: | 0 | 4855 | 14.39 | 1.0 | 0.6 | 9.30 | 229 | KP |
| 1044 | UGC 12840 | 23 54 30.1 | +28 52 21 | (R)SAB | 1 | 6856 | 14.06 | 1.2 | 1.1 | 9.68 | 236 | KP |
| 1047 | UGC 12857 | 23 56 47.5 | +01 21 19 | Sbc: sp | 0 | 2459 | 14.49 | 1.8 | 0.4 | 9.57 | 265 | S |

channel width of 2 MHz. Each 6-min scan began by a chopper wheel calibration on a load at ambient temperature, with a chopper wheel calibration on a cold load every two scans.

The IRAM observations were carried out in good weather conditions. Pointing was checked using continuum sources every 90 min, with an average error of 3 arcsec rms. We used two SIS receivers in parallel and two 512×1 MHz backends and the autocorrelator as back ends. $T_{\rm sys}$ was of the order 280−330 K. We used a wobbler switching procedure, with a wobbler throw of 4′ in azimuth. Each 6-min scan began by a chopper wheel calibration on a load at ambient temperature and a cold load.

Galaxies were all observed at their nominal coordinates listed in Table 1. Twenty-eight among the largest-brightest optical sources were mapped, with one beam sampling along the major axis for inclined galaxies or along major and minor axis for face-on objects. The total integration time was on average 120 min on+off (i.e. 60 min on the source) per position, yielding rms noise levels of about 4 mK (in the $T_{\rm mb}$ scale) at the SEST, 2 at Kitt Peak and 6 at IRAM, after velocity smoothing to 15 km s$^{-1}$. The baselines were flat owing to the use of beam-switching, thereby requiring that only linear baselines be subtracted. The antenna temperature $T_{\rm A}^*$ (SEST, IRAM) and $T_{\rm R}^*$ (Kitt Peak) were corrected for telescope and atmospheric losses. In the following analysis we use the main-beam brightness temperature scale, $T_{\rm mb}$, with $T_{\rm mb} = T_{\rm A}^*/0.69$ at the SEST, $T_{\rm mb} = T_{\rm A}^*/0.56$ at IRAM and $T_{\rm mb} = T_{\rm R}^*/0.84$ (where the main beam efficiency is $\eta_{\rm mb} = 0.54$ and the forward scattering and spillover efficiency $\eta_{\rm fss} = 0.68$) at Kitt Peak. This scale is appropriate for sources with sizes comparable to, or smaller than the beam size. These main-beam temperatures can be converted into flux densities using 27 Jy/K at the SEST, 29 Jy/K at Kitt Peak and 4.4 Jy/K at IRAM.

## 4. Results

### 4.1. Results of our observations

The $^{12}$CO(1–0) spectra of all the detected galaxies were reduced with the CLASS package (Forveille et al. 1990): the observational results are listed in Table 2 (also available in electronic form at the CDS). All data are given in the $T_{\rm mb}$ scale. Of the 99 observed galaxies 30 were not detected. Table 2 is arranged as follows:

- Column 1: KIG name.
- Columns 2 and 3: offset position, in arcsec.
- Column 4: rms noise, in mK.
- Column 5: intensity of the $I$(CO) line ($I(\mathrm{CO}) = \int T_{\rm mb}{\rm d}v$) in K km s$^{-1}$ (first line moment definition)). For undetected galaxies, the reported value is an upper limit determined as follows:

$$I(\mathrm{CO}) = 2\sigma(\Delta V_{\rm HI}\delta V_{\rm CO})^{1/2}\ \mathrm{K\ km\ s^{-1}} \quad (1)$$

where $\sigma$ is the rms noise of the spectrum, $\Delta V_{\rm HI}$ is the HI line width, and $\delta V_{\rm CO}$ is the spectral resolution (for galaxies with $\Delta V_{\rm HI}$ not available, the HI width has been determined assuming a standard $\Delta V_{\rm HI} = 300\sin(i)$ km s$^{-1}$, where $i$ is the galaxy inclination or $\Delta V_{\rm HI} = 50$ km s$^{-1}$ if $i = 0$). $\delta V_{\rm CO} = 15$ km s$^{-1}$. For undetected pointings in mapped galaxies, we estimate a conservative upper limit using $\Delta V_{\rm HI}$ in Eq. (1), since generally $\Delta V_{\rm HI} > \Delta V_{\rm CO}$. The error on the intensity of the CO line, $\Delta I$(CO), is computed as:

$$\Delta I(\mathrm{CO}) = 2\sigma(\Delta V_{\rm CO}\delta V_{\rm CO})^{1/2}\ \mathrm{K\ km\ s^{-1}} \quad (2)$$

where $\sigma$ is the rms noise of the spectrum, $\Delta V_{\rm CO}$ is the CO linewidth (given in Col. 7), and $\delta V_{\rm CO}$ is the spectral resolution[3]. Spectra were smoothed to $\delta V_{\rm CO} = 15$ km s$^{-1}$.
- Column 6: heliocentric velocity determined from the CO line (second line moment), in km s$^{-1}$ (optical definition $v = cz = \Delta\lambda/\lambda_0$). The estimated error is comparable to the resolution, thus ∼15 km s$^{-1}$.
- Column 7: width at 50% of the maximum intensity of the CO line, in km s$^{-1}$, with an estimated error of ∼15−20 km s$^{-1}$.
- Column 8: notes: *m* stands for marginally detected galaxies, *a* for nearby galaxies whose distance determination from redshift measurements are highly inaccurate ($v_{\rm hel} \leq 1000$ km s$^{-1}$).
- Column 9: filling factor, defined as the ratio of the beam area to the optical surface of the galaxy. For mapped galaxies the beam area is the total mapped area, including detected and undetected positions.
- Column 10: the $M(H_2)_{\rm CO}$ mass (or upper limit), determined adopting a standard $X$ conversion factor $X = 2.3 \times 10^{20}$ mol cm$^{-2}$ (K km s$^{-1}$)$^{-1}$ (Strong et al. 1988):

$$M(\mathrm{H_2})_{\rm CO} = 68.08 \times (D/\mathrm{Mpc})^2 I(\mathrm{CO})\left(\mathrm{K\ km\ s^{-1}}\right)(\theta/1'')^2 \quad (3)$$

where in mapped galaxies $I$(CO) is the sum of the intensities $I_i$(CO) of each detected beam position given in Col. 5 of Table 2, $I(\mathrm{CO}) = \sum_{i=1}^{n} I_i(\mathrm{CO})$ (K km s$^{-1}$). The distance is determined from redshif measurements assuming $H_0 = 75$ km s$^{-1}$ Mpc$^{-1}$;
- Column 11: the molecular gas mass determined from the CO line intensity assuming the $M_{\rm B}$ absolute magnitude-dependent $X$ conversion factor given in Table 5 of Boselli et al. (2002).

### 4.2. Comparison with previous observations

Two galaxies: KIG 652 and KIG 906, have been observed both at the SEST and at Kitt Peak. The Kitt Peak observations of

[3] Both Eqs. (1) and (2) assume that the uncertainty is due to noise in the spectrum, ignoring the error on the determination of the baseline. As suggested by Sage (1993) this uncertainty can be taken into account by combining in quadratic sum the error due to noise in the spectrum ($\Delta I(\mathrm{CO})_{\rm noise} = \sigma\ (\Delta V_{\rm CO}\ \delta V_{\rm CO})^{1/2}$) to that in the determination of the baseline $\Delta I(\mathrm{CO})_{\rm baseline} = \sigma\ \Delta V_{\rm CO}\ (\delta V_{\rm CO}/\Delta V_{\rm baseline})^{1/2}$, where $\Delta V_{\rm baseline}$ is the velocity range over which the baseline is fitted. Since $\Delta V_{\rm baseline} < \Delta V_{\rm CO}$ for all the observed galaxies ($\Delta V_{\rm CO}$ is always <500 km s$^{-1}$, for a bandwidth of ∼1300 km s$^{-1}$ for the Kitt Peak and IRAM observations, and significantely larger at the SEST), it results that $\sqrt{\Delta I(\mathrm{CO})^2_{\rm noise} + \Delta I(\mathrm{CO})^2_{\rm baseline}} < \Delta I(\mathrm{CO})/\sqrt{2}$, where $\Delta I$(CO) is the value given in Eq. (2). Thus our error determination, even though it does not exactly corresponds to a "two $\sigma$ error", is more conservative than a "one $\sigma$ error" obtained taking into account the uncertainty due to the baseline determination.

**Table 2.** Results of the observations, in $T_{mb}$ scale.

| KIG | Offset arcsec | Offset arcsec | rms mK | $I$(CO) K km s$^{-1}$ | $V$(CO) km s$^{-1}$ | $\Delta V_{CO}$ km s$^{-1}$ | Notes | $FF$ | log $M(H_2)_{CO}$ $M\odot$ | log $M(H_2)$ $M\odot$ |
|---|---|---|---|---|---|---|---|---|---|---|
| (1) | (2) | (3) | (4) | (5) | (6) | (7) | (8) | (9) | (10) | (11) |
| 1 | 0 | 0 | 4.1 | 1.99 ± 0.55 | 7322 | 302 | m | 0.32 | 9.37 | 9.01 |
| 4 | 0 | 0 | 2.7 | 5.71 ± 0.36 | 2345 | 292 | | 0.27 | 9.05 | 8.88 |
| 6 | 0 | 0 | 2.1 | <0.21 | | | | 0.92 | <8.19 | <8.08 |
| 11 | 0 | 0 | 3.9 | <0.51 | | | | 0.24 | <8.26 | <8.22 |
| 22 | 0 | 0 | 3.1 | 0.94 ± 0.31 | 13131 | 166 | | 0.17 | 9.55 | 9.02 |
| 33 | 0 | 0 | 4.6 | 3.53 ± 0.56 | 4156 | 243 | | 1.78 | 9.14 | 8.94 |
| 33 | –41 | 11 | 11.0 | <1.47 | | | | | | |
| 33 | –41 | –11 | 11.0 | <1.47 | | | | | | |
| 33 | 41 | –11 | 11.0 | <1.47 | | | | | | |
| 33 | 41 | 11 | 11.0 | <1.47 | | | | | | |
| 45 | 0 | 0 | 2.9 | <0.19 | | | a | 0.78 | <5.23 | <6.41 |
| 53 | 0 | 0 | 3.4 | 1.25 ± 0.27 | 3125 | 104 | | 0.31 | 8.65 | 8.52 |
| 56 | 0 | 0 | 3.0 | 1.18 ± 0.41 | 5142 | 317 | m | 0.22 | 8.85 | 8.57 |
| 59 | 0 | 0 | 5.6 | 1.07 ± 0.69 | 4357 | 250 | | 0.45 | 9.46 | 9.31 |
| 59 | –37 | 22 | 7.7 | <0.87 | | | | | | |
| 59 | –22 | –37 | 7.7 | <0.87 | | | | | | |
| 59 | 22 | 37 | 9.8 | 1.69 ± 0.64 | 4450 | 71 | | | | |
| 59 | 37 | –22 | 12.0 | 4.22 ± 1.36 | 4148 | –1 | m | | | |
| 68 | 0 | 0 | 5.8 | <0.60 | | | | 0.56 | <7.60 | <7.55 |
| 68 | –31 | –31 | 10.5 | <1.08 | | | | | | |
| 68 | –31 | 31 | 10.5 | <1.08 | | | | | | |
| 68 | 31 | 31 | 10.5 | <1.08 | | | | | | |
| 68 | 31 | –31 | 10.5 | <1.08 | | | | | | |
| 72 | 0 | 0 | 3.6 | 1.80 ± 0.47 | 5160 | 287 | | 0.40 | 9.04 | 8.84 |
| 87 | 0 | 0 | 2.5 | 0.41 ± 0.26 | 5652 | 181 | m | 1.28 | 8.47 | 8.31 |
| 94 | 0 | 0 | 2.0 | 0.44 ± 0.29 | 4770 | 347 | m | 2.10 | 8.57 | 8.50 |
| 115 | 0 | 0 | 7.2 | <0.95 | | | | 0.54 | <8.75 | <8.63 |
| 123 | 0 | 0 | 5.5 | 1.40 ± 0.66 | 5910 | 242 | | 0.18 | 9.04 | 8.69 |
| 139 | 0 | 0 | 7.0 | <0.70 | | | | 0.48 | <7.07 | <7.34 |
| 139 | 8 | 42 | 5.1 | <0.51 | | | | | | |
| 139 | –8 | –42 | 4.3 | <0.43 | | | | | | |
| 153 | 0 | 0 | 5.5 | <0.64 | | | | 0.34 | 8.15 | 8.06 |
| 153 | –15 | 13 | 6.7 | <0.78 | | | | | | |
| 153 | 15 | –13 | 6.0 | 1.57 ± 0.64 | – | – | m | | | |
| 155 | 0 | 0 | 3.2 | 1.32 ± 0.20 | 1570 | 63 | | 0.69 | 8.07 | 8.13 |
| 166 | 0 | 0 | 4.5 | 2.84 ± 0.60 | 5005 | 297 | | 0.19 | 8.64 | 8.43 |
| 166 | –10 | 17 | 11.6 | <1.96 | | | | | | |
| 166 | 10 | –17 | 10.0 | <1.69 | | | | | | |
| 176 | 0 | 0 | 2.1 | 0.79 ± 0.26 | 4993 | 250 | | 0.59 | 8.85 | 8.59 |
| 180 | 0 | 0 | 2.0 | 0.63 ± 0.12 | 982 | 63 | | 0.29 | 7.34 | 7.55 |
| 191 | 0 | 0 | 1.6 | 0.67 ± 0.23 | 6025 | 334 | m | 1.17 | 8.93 | 8.66 |
| 278 | 0 | 0 | 1.8 | <0.30 | | | | 1.91 | <8.82 | <8.54 |
| 279 | 0 | 0 | 5.4 | <0.59 | | | | 0.92 | <7.70 | <7.73 |
| 279 | –11 | 44 | 4.6 | <0.51 | | | | | | |
| 279 | 11 | –44 | 8.5 | <0.93 | | | | | | |
| 291 | 0 | 0 | 3.1 | 0.72 ± 0.18 | 2531 | 54 | | 0.44 | 7.43 | 7.48 |
| 291 | –20 | 0 | 10.0 | <0.97 | | | | | | |
| 291 | 0 | 20 | 8.6 | <0.83 | | | | | | |
| 291 | 0 | –20 | 10.0 | <0.97 | | | | | | |
| 291 | 20 | 0 | 8.1 | <0.79 | | | | | | |
| 298 | 0 | 0 | 1.2 | 0.99 ± 0.13 | 7052 | 208 | | 0.35 | 9.26 | 8.91 |
| 300 | 0 | 0 | 5.7 | <0.53 | | | | 0.35 | 7.07 | 7.40 |
| 300 | 16 | –12 | 6.3 | <0.58 | | | | | | |
| 300 | –16 | 12 | 6.5 | 0.96 ± 0.60 | – | – | m | | | |
| 303 | 0 | 0 | 6.8 | <0.83 | | | | 0.67 | <8.49 | <8.19 |
| 303 | –41 | 13 | 11.0 | <1.34 | | | | | | |
| 303 | 41 | –13 | 7.3 | <0.79 | | | | | | |
| 339 | 0 | 0 | 2.2 | 1.20 ± 0.23 | 7541 | 188 | | 0.43 | 9.40 | 9.06 |

**Table 2.** continued.

| KIG | Offset arcsec | Offset arcsec | rms mK | $I$(CO) K km s$^{-1}$ | $V$(CO) km s$^{-1}$ | $\Delta V_{CO}$ km s$^{-1}$ | Notes | $FF$ | log $M(H_2)_{CO}$ $M\odot$ | log $M(H_2)$ $M\odot$ |
|---|---|---|---|---|---|---|---|---|---|---|
| (1) | (2) | (3) | (4) | (5) | (6) | (7) | (8) | (9) | (10) | (11) |
| 343 | 0 | 0 | 3.3 | 2.37 ± 0.31 | 5362 | 151 | m | 0.22 | 9.18 | 8.89 |
| 359 | 0 | 0 | 2.5 | <0.40 | | | | 0.71 | <8.34 | <8.01 |
| 359 | –28 | –33 | 6.7 | <1.08 | | | | | | |
| 359 | 28 | 33 | 6.7 | <1.08 | | | | | | |
| 363 | 0 | 0 | 2.4 | 2.43 ± 0.33 | 3041 | 312 | | 0.58 | 8.92 | 8.77 |
| 383 | 0 | 0 | 6.2 | 1.41 ± 0.49 | 1498 | 105 | | 0.50 | 7.85 | 7.93 |
| 383 | –18 | –39 | 9.1 | <1.00 | | | | | | |
| 383 | 18 | 39 | 9.1 | <1.00 | | | | | | |
| 401 | 0 | 0 | 2.8 | <0.44 | | | | 1.03 | <8.61 | <8.30 |
| 443 | 0 | 0 | 5.3 | <0.67 | | | | 1.61 | <8.71 | <8.58 |
| 444 | 0 | 0 | 4.7 | 3.17 ± 0.24 | 4474 | 45 | | 0.80 | 9.15 | 8.88 |
| 464 | 0 | 0 | 4.8 | 1.15 ± 0.57 | 1462 | 235 | m | 2.03 | 8.34 | 8.59 |
| 464 | –35 | –25 | 10.0 | 1.51 ± 1.00 | 1509 | 168 | m | | | |
| 464 | 35 | 25 | 7.0 | 2.20 ± 0.76 | 1578 | – | m | | | |
| 489 | 0 | 0 | 3.3 | 2.61 ± 0.37 | 5980 | 205 | | 1.26 | 8.73 | 8.58 |
| 489 | 0 | –20 | 7.2 | <0.80 | | | | | | |
| 489 | 0 | 20 | 6.6 | <0.73 | | | | | | |
| 491 | 0 | 0 | 4.7 | <0.44 | | | | 0.54 | <8.57 | <8.41 |
| 492 | 0 | 0 | 3.5 | <0.58 | | | | 1.07 | <8.58 | <8.48 |
| 499 | 0 | 0 | 4.4 | 5.61 ± 0.66 | 8624 | 380 | | 0.67 | 9.71 | 9.40 |
| 499 | –19 | –6 | 7.2 | 0.75 ± 1.21 | 8401 | – | m | | | |
| 499 | 19 | 6 | 7.6 | 1.31 ± 1.28 | – | – | m | | | |
| 500 | 0 | 0 | 3.5 | <0.46 | | | | 0.19 | <8.56 | <8.21 |
| 502 | 0 | 0 | 4.0 | 1.18 ± 0.26 | 1785 | 70 | m | 0.48 | 7.90 | 8.32 |
| 502 | –15 | –40 | 8.4 | <0.97 | | | | | | |
| 502 | 15 | 40 | 9.1 | <1.05 | | | | | | |
| 509 | 0 | 0 | 4.9 | <0.60 | | | | 1.51 | 8.43 | 8.52 |
| 509 | 9 | –42 | 7.0 | <0.85 | | | | | | |
| 509 | –9 | 42 | 7.0 | 2.10 ± 0.36 | 3118 | 45 | m | | | |
| 512 | 0 | –20 | 6.6 | 1.36 ± 0.65 | 1924 | 162 | | 0.11 | 8.07 | 8.06 |
| 512 | 0 | 20 | 6.7 | <0.70 | | | | | | |
| 512 | 20 | 0 | 7.4 | <0.77 | | | | | | |
| 512 | 0 | 0 | 3.5 | 0.99 ± 0.35 | 1924 | 162 | | | | |
| 512 | –20 | 0 | 7.3 | 3.24 ± 0.83 | 1885 | 216 | | | | |
| 527 | 0 | 0 | 5.5 | 4.32 ± 0.73 | 2033 | 297 | | 0.69 | 8.71 | 8.66 |
| 527 | –28 | 33 | 7.7 | <1.16 | | | | | | |
| 527 | 28 | –33 | 7.7 | 1.44 ± 0.69 | 2168 | 135 | | | | |
| 540 | 0 | 0 | 3.0 | <0.33 | | | | 1.14 | <7.69 | <7.80 |
| 545 | 0 | 0 | 1.9 | 1.87 ± 0.29 | 4666 | 375 | | 0.56 | 9.17 | 8.99 |
| 547 | 0 | 0 | 2.5 | 0.65 ± 0.15 | 931 | 62 | | 0.30 | 7.34 | 7.63 |
| 604 | 0 | 0 | 4.0 | 5.38 ± 0.56 | 1717 | 332 | | 0.12 | 8.42 | 8.29 |
| 604 | –20 | 0 | 6.0 | <0.90 | | | | | | |
| 604 | 0 | 20 | 8.7 | <1.31 | | | | | | |
| 604 | 0 | –20 | 7.0 | <1.05 | | | | | | |
| 604 | 7 | 19 | 6.3 | <0.95 | | | | | | |
| 604 | 20 | 0 | 9.6 | <1.44 | | | | | | |
| 604 | –7 | –19 | 9.2 | 8.64 ± 1.32 | 1776 | 345 | | | | |
| 605 | 0 | 0 | 2.2 | 0.78 ± 0.18 | 2439 | 106 | | 0.09 | 8.21 | 8.00 |
| 626 | 0 | 0 | 2.9 | 1.14 ± 0.26 | 1640 | 136 | m | 0.06 | 7.83 | 7.81 |
| 638 | 0 | 0 | 5.0 | 4.60 ± 0.60 | 1813 | 243 | | 0.45 | 8.76 | 8.69 |
| 638 | 26 | –34 | 7.7 | <1.02 | | | | | | |
| 638 | –26 | 34 | 7.7 | 3.80 ± 0.48 | 1832 | 65 | | | | |
| 652 | 0 | 0 | 3.5 | 1.39 ± 0.38 | 1931 | 196 | | 0.58 | 8.51 | 8.60 |
| 652 | –37 | –22 | 6.1 | <0.64 | | | | | | |
| 652 | 37 | 22 | 6.8 | 0.52 ± 0.71 | – | – | m | | | |
| 653 | 0 | 0 | 1.9 | 0.83 ± 0.33 | 4982 | 495 | | 0.31 | 8.86 | 8.59 |
| 669 | 0 | 0 | 5.2 | 2.63 ± 0.73 | 1922 | 330 | m | 0.84 | 8.83 | 8.95 |
| 669 | 0 | 40 | 18.0 | <2.59 | | | | | | |
| 669 | 20 | 0 | 11.0 | <1.58 | | | | | | |
| 669 | –20 | 0 | 11.4 | 2.84 ± 1.64 | – | – | m | | | |
| 669 | 0 | 20 | 9.3 | 6.92 ± 1.19 | 2265 | 272 | | | | |

**Table 2.** continued.

| KIG | Offset arcsec | Offset arcsec | rms mK | $I$(CO) K km s$^{-1}$ | $V$(CO) km s$^{-1}$ | $\Delta V_{CO}$ km s$^{-1}$ | Notes | $FF$ | log $M(H_2)_{CO}$ $M\odot$ | log $M(H_2)$ $M\odot$ |
|---|---|---|---|---|---|---|---|---|---|---|
| (1) | (2) | (3) | (4) | (5) | (6) | (7) | (8) | (9) | (10) | (11) |
| 669 | 0 | –40 | 8.7 | 6.94 ± 1.21 | 1950 | 324 | | | | |
| 669 | 0 | –20 | 9.0 | 9.14 ± 1.45 | 1991 | 432 | | | | |
| 695 | 0 | 0 | 3.4 | 0.91 ± 0.29 | 10549 | 121 | | 1.07 | 9.35 | 8.95 |
| 712 | 0 | 0 | 2.7 | 1.72 ± 0.29 | 1853 | 186 | | 0.27 | 8.34 | 8.27 |
| 772 | 0 | 0 | 1.7 | 1.40 ± 0.15 | 5152 | 125 | | 0.38 | 8.65 | 8.57 |
| 785 | 0 | 0 | 1.8 | <0.29 | | | | 0.48 | <8.78 | <8.40 |
| 786 | 0 | 0 | 3.1 | 1.84 ± 0.35 | 6299 | 211 | | 1.71 | 9.21 | 9.03 |
| 791 | 0 | 0 | 3.5 | 0.92 ± 0.33 | 2589 | 151 | m | 1.17 | 8.13 | 8.31 |
| 800 | 0 | 0 | 2.7 | 1.78 ± 0.38 | 6150 | 332 | | 0.61 | 9.18 | 8.97 |
| 808 | 0 | 0 | 3.8 | 0.32 ± 0.26 | 1687 | 76 | m | 0.37 | 7.82 | 7.93 |
| 808 | –45 | 0 | 7.3 | <0.65 | | | | | | |
| 808 | 45 | 0 | 7.3 | <0.65 | | | | | | |
| 808 | 0 | 45 | 6.6 | 0.33 ± 0.59 | 1657 | – | m | | | |
| 808 | 0 | –45 | 7.3 | 0.39 ± 0.65 | – | – | m | | | |
| 812 | 0 | 0 | 3.9 | 2.28 ± 0.57 | 3141 | 352 | | 0.16 | 8.91 | 8.67 |
| 840 | 0 | 0 | 2.0 | 1.58 ± 0.22 | 4787 | 196 | | 0.51 | 9.12 | 8.80 |
| 850 | 0 | 0 | 3.5 | 11.40± 0.39 | 1503 | 209 | | 0.12 | 8.96 | 8.82 |
| 851 | 0 | 0 | 2.5 | <0.26 | | | | 0.15 | <7.50 | <7.51 |
| 862 | 0 | 0 | 3.1 | 3.00 ± 0.33 | 4682 | 188 | | 0.50 | 9.38 | 9.14 |
| 879 | 0 | 0 | 4.1 | <0.55 | | | | 0.73 | <8.29 | <8.27 |
| 886 | 0 | 0 | 2.5 | <0.30 | | | | 0.86 | <8.05 | <7.93 |
| 889 | 0 | 0 | 2.6 | <0.42 | | | | 1.56 | <8.31 | <8.28 |
| 890 | 0 | 0 | 2.7 | 4.31 ± 0.47 | 4799 | 498 | | 0.24 | 9.56 | 9.33 |
| 897 | 0 | 0 | 2.2 | <0.42 | | | | 0.34 | <8.57 | <8.31 |
| 906 | 0 | 0 | 4.2 | 2.30 ± 0.52 | 4946 | 257 | | 2.70 | 9.09 | 9.01 |
| 906 | –23 | –36 | 3.8 | <0.61 | | | | | | |
| 906 | 23 | 36 | 3.8 | <0.61 | | | | | | |
| 910 | 0 | 0 | 1.5 | <0.24 | | | | 1.31 | <8.33 | <8.17 |
| 911 | 0 | 0 | 4.3 | 2.94 ± 0.70 | 5329 | 438 | m | 0.57 | 9.28 | 8.99 |
| 930 | 0 | 0 | 3.7 | <0.55 | | | | 0.41 | <8.44 | <8.32 |
| 935 | 0 | 0 | 6.1 | 3.10 ± 0.41 | 3967 | 76 | | 1.15 | 9.04 | 8.76 |
| 935 | –42 | 11 | 5.6 | <0.43 | | | | | | |
| 935 | –15 | 40 | 8.5 | <0.66 | | | | | | |
| 935 | 15 | –40 | 8.1 | <0.63 | | | | | | |
| 935 | 42 | –11 | 5.6 | <0.43 | | | | | | |
| 940 | 0 | 0 | 3.3 | 4.70 ± 0.44 | 8051 | 302 | | 0.67 | 9.83 | 9.52 |
| 949 | 0 | 0 | 9.1 | <0.85 | | | | 0.43 | <7.73 | <8.00 |
| 976 | 0 | 0 | 2.5 | 3.05 ± 0.33 | 2844 | 292 | | 0.60 | 8.95 | 8.96 |
| 984 | 0 | 0 | 1.7 | <0.31 | | | | 1.40 | <8.78 | <8.54 |
| 985 | 0 | 0 | 3.8 | <0.44 | | | | 0.11 | <7.56 | <7.65 |
| 1001 | 0 | 0 | 3.8 | 1.02 ± 0.52 | – | – | m | 0.49 | 8.33 | 8.20 |
| 1001 | –15 | 40 | 7.7 | <1.06 | | | | | | |
| 1001 | 15 | –40 | 7.7 | <1.06 | | | | | | |
| 1003 | 0 | 0 | 3.2 | 1.56 ± 0.42 | 3475 | 287 | | 1.51 | 8.62 | 8.68 |
| 1006 | 0 | 0 | 2.0 | 1.65 ± 0.21 | 5465 | 181 | | 1.75 | 9.26 | 9.10 |
| 1009 | 0 | 0 | 1.5 | 0.71 ± 0.16 | 4871 | 195 | m | 0.67 | 8.79 | 8.50 |
| 1013 | 0 | 0 | 1.6 | 2.67 ± 0.27 | 5011 | 478 | | 1.75 | 9.41 | 9.23 |
| 1019 | 0 | 0 | 4.2 | 2.98 ± 0.56 | 3485 | 292 | | 0.75 | 9.12 | 8.94 |
| 1023 | 0 | 0 | 1.3 | 0.82 ± 0.13 | 8042 | 166 | | 0.29 | 9.29 | 8.89 |
| 1027 | 0 | 0 | 6.2 | <0.86 | | | | 0.76 | <8.72 | <8.54 |
| 1028 | 0 | 0 | 2.0 | 0.82 ± 0.19 | 3066 | 151 | | 1.17 | 8.45 | 8.38 |
| 1036 | 0 | 0 | 2.8 | 1.73 ± 0.28 | 4264 | 166 | | 0.84 | 9.06 | 8.89 |
| 1038 | 0 | 0 | 1.8 | 0.94 ± 0.21 | 5023 | 229 | | 0.16 | 8.92 | 8.66 |
| 1039 | 0 | 0 | 2.6 | 0.85 ± 0.29 | 4860 | 208 | m | 1.40 | 8.87 | 8.73 |
| 1044 | 0 | 0 | 1.9 | 0.22 ± 0.12 | 6850 | 63 | m | 0.64 | 8.58 | 8.25 |
| 1047 | 0 | 0 | 5.0 | <0.63 | | | | 2.14 | <7.93 | <8.08 |
| 1047 | –24 | –25 | 5.6 | <0.71 | | | | | | |
| 1047 | 24 | 35 | 5.6 | <0.71 | | | | | | |

**Table 3.** Comparison of the Kitt Peak observations with those available from other telescopes.

| KIG | $a$ | $b$ | $I(\mathrm{CO})_{\mathrm{KP}}$ | $I(\mathrm{CO})_{\mathrm{lit}}$ | $\theta_{\mathrm{lit}}$ | Ref. | $(\theta_{\mathrm{lit}}/\theta_{\mathrm{KP}})^2$ | expected $I(\mathrm{CO})_{\mathrm{KP}}$ | CO distribution |
|---|---|---|---|---|---|---|---|---|---|
| | ′ | ′ | K km s$^{-1}$ | K km s$^{-1}$ | arcsec | | | K km s$^{-1}$ | |
| (1) | (2) | (3) | (4) | (5) | (6) | (7) | (8) | (9) | (10) |
| 4 | 3.5 | 0.9 | 5.71 ± 0.33 | 9.49 ± 1.44 | 45 | 2 | 0.67 | 6.35 | point-like |
| 547 | 2.0 | 1.4 | 0.65 ± 0.16 | 2.58 ± 0.91 | 45 | 2 | 0.67 | 1.73 | point-like |
| 652 | 1.9 | 1.4 | 1.45 ± 0.50 | 3.20 ± 0.38 | 43 | 1 | 0.61 | 1.96 | point-like |
| 906 | 1.9 | 0.3 | 2.10 ± 0.50 | 2.30 ± 0.52 | 43 | 1 | 0.61 | 1.41 | extended |
| 850 | 3.8 | 1.9 | 11.40 ± 0.36 | 10.00 ± - | 55 | 3 | 1.00 | 10.00 | extended |
| 850 | 3.8 | 1.9 | 11.40 ± 0.36 | 30.00 ± 5.80 | 33 | 4 | 0.36 | 10.80 | extended |
| 850 | 3.8 | 1.9 | 11.40 ± 0.36 | 13.80 ± 1.67 | 43 | 2 | 0.61 | 8.44 | extended |

Column 1: KIG name.
Columns 2 and 3: major and minor optical diameters, in arcmin.
Column 4: $I$(CO) intensity and error at Kitt Peak.
Column 5: $I$(CO) intensity and error at other telescopes.
Column 6: beamsize of the telescope.
Column 7: references: 1: SEST observations (this work); 2: FCRAO (Young et al. 1995); 3: Kitt Peak (Solomon & Sage 1988); 4: Onsala (Elfhag et al. 1996).
Column 8: ratio of the mapped areas.
Column 9: expected $I$(CO) intensity in a 55 arcsec beam for a point-like source estimated from CO data available in the literature, *expected* $I(\mathrm{CO})_{\mathrm{KP}} = I(\mathrm{CO})_{\mathrm{lit}} \times (\theta_{\mathrm{lit}}/\theta_{\mathrm{KP}})^2$.
Column 10: expected CO distribution.

KIG 652 gives $I(\mathrm{CO}) = 1.45 \pm 0.50$ K km s$^{-1}$, while the SEST one $I(\mathrm{CO}) = 3.20 \pm 0.38$ K km s$^{-1}$. For KIG 906, Kitt Peak observations gives $I(\mathrm{CO}) = 2.10 \pm 0.50$ K km s$^{-1}$, while the SEST one $I(\mathrm{CO}) = 2.30 \pm 0.52$ K km s$^{-1}$.

Three galaxies of our sample have published CO data:

KIG 4, NGC 7817: our Kitt Peak observation gives $I(\mathrm{CO}) = 5.71 \pm 0.33$ K km s$^{-1}$, while Young et al. (1995), using the FCRAO 14.7 m telescope, obtained $I(\mathrm{CO}) = 9.49 \pm 1.44$ K km s$^{-1}$ (main beam scale) in the central position.

KIG 547, NGC 4635: our Kitt Peak observation gives $I(\mathrm{CO}) = 0.65 \pm 0.16$ K km s$^{-1}$, while Young et al. (1995), still with the FCRAO 14.7 m telescope, obtained $I(\mathrm{CO}) = 2.58 \pm 0.91$ K km s$^{-1}$ (main beam scale).

KIG 850, NGC 6643: three independent measurements are available in the literature: Young et al. (1995), with the FCRAO 14.7 m telescope, obtained $I(\mathrm{CO}) = 13.80 \pm 1.67$ K km s$^{-1}$, Solomon & Sage (1988), with the Kitt Peak 12 m telescope, measured $I(\mathrm{CO}) = 10.0$ K km s$^{-1}$, and Elfhag et al. (1996) $I(\mathrm{CO}) = 30.0 \pm 5.8$ K km s$^{-1}$ using the Onsala 20 m telescope. These values (all given in main beam scale) must be compared with our Kitt Peak observation $I(\mathrm{CO}) = 11.40 \pm 0.36$ K km s$^{-1}$.

A direct comparison of the various sets of data is not straightforward because of the different beam sizes of the telescopes ($HPBW = 55$ arcsec for Kitt Peak, 43 arcsec for the SEST, 45 arcsec for the FCRAO and 33 arcsec for Onsala). The two independent observations of KIG 850 carried out with the same telescope give consistent results within 15%. As shown in Table 3, the other sets of data are consistent with ours for a point-like emission in the galaxies KIG 4 and 652, and for an extended and radially declining emission in KIG 906 and 850[4]. The only inconsistent data are that of KIG 547, whose $I$(CO) intensity measured at Kitt Peak is too small compared to that obtained at the FCRAO even in the case of a point-like CO distribution. We thus conclude that our observations are generally consistent, within the errors, with those available in the literature.

### 4.3. Statistical properties of the sample

Since the physical properties of the ISM strongly depend on the metallicity and on the UV radiation field, the use of a constant CO to $H_2$ conversion factor is no more justified for a sample of galaxies spanning a wide range in morphological type (from giant spirals to dwarf irregulars) and luminosity ($-21.2 \leq M_{\mathrm{B}} \leq -17.3$) as the one observed in this work (Boselli et al. 2002). As shown by Boselli et al. (2002), in this luminosity range $X$ varies by a factor of ∼5. To avoid any systematic bias, the statistical properties on the molecular gas content of this sample of galaxies can be estimated only using a luminosity dependent conversion factor. Indeed the molecular

[4] All sources are undersampled in both sets of observations. Because of dilution effects, for sources whose CO emission is less extended than the angular dimension of the smaller beam (here defined as point-like sources), the CO intensity observed in the larger beam (Kitt Peak observations) should equal that observed in the smaller beam multiplyed by the ratio of the smaller to larger mapped areas. In CO extended sources, independently on the CO distribution within the disc of the galaxy, the CO intensity observed in the larger beam overcomes that observed in the smaller beam multiplied by a similar geometrical correction factor.

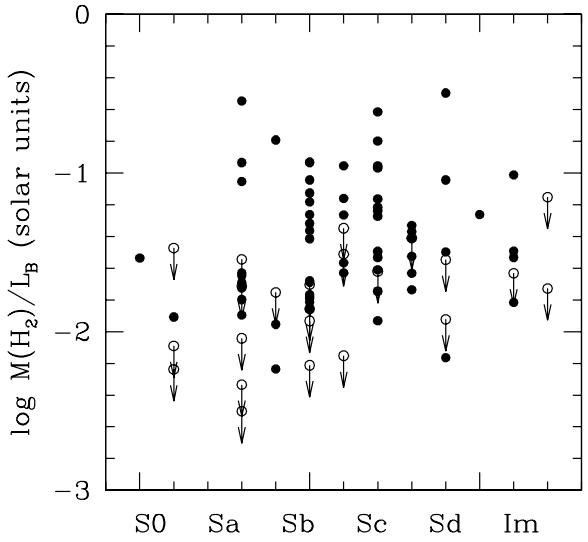


**Fig. 2.** The molecular gas mass to optical blue luminosity of the target galaxies. Filled symbols are for detected galaxies, arrows are upper limits to the $M(H_2)/L_B$ ratio (CO undetected galaxies).

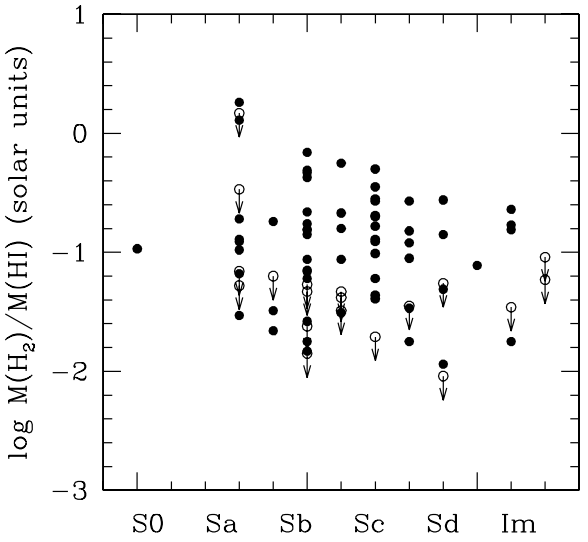


**Fig. 3.** The molecular to atomic gas mass ratio as a function of the morphological type. Filled symbols are for detected galaxies, arrows are upper limits to the $M(H_2)/M(HI)$ ratio (CO undetected galaxies).

gas mass determined assuming a constant CO to $H_2$ conversion factor is overestimated in massive, early-type spirals, and underestimated in low-luminosity, dwarf galaxies.

Assuming a luminosity-dependent CO to $H_2$ conversion factor we can trace the molecular gas mass to optical luminosity ratio (Fig. 2) and the molecular to atomic gas ratio (Fig. 3) vs. morphological type of the sample galaxies.

The molecular gas mass to optical luminosity seems to increase from early-type to late-type spirals, consistently with what observed by Boselli et al. (1997) using *H* band luminosities[5].

Consistent with Boselli et al. (2002), we find that in the isolated galaxy sample the molecular gas fraction is ∼18% of the HI gas (if upper limits are treated as detections).

*Acknowledgements.* We want to thank the 12 m telescope operators for their invaluable help during the remote observations, and the SEST and IRAM operators for their assistance. We thank J. Iglesias for his help in preparation of the Tables. This research has made use of NASA extragalactic Database (NED) and on the LEDA Database.

[5] The *H* band luminosity, compared to the *B* band luminosity, is unaffected by dust and by recent events of star formation and is a direct tracer of the total mass (Gavazzi et al. 1996).

## References

Boselli, A. 1994, A&A, 292, 1
Boselli, A., Gavazzi, G., Lequeux, J., et al. 1997, A&A, 327, 522
Boselli, A., Gavazzi, G., Donas, J., & Scodeggio, M. 2001, AJ, 121, 753
Boselli, A., Lequeux, J., & Gavazzi, G. 2002, A&A, 384, 33
Casoli, F., Boissé P., Combes, F., & Dupraz, C. 1991, A&A, 249, 359
Casoli, F., Sauty, S., Gerin, M., et al. 1998, A&A, 331, 451
Elfhag, T., Booth, R., Hoglund, B., et al. 1996, A&AS, 115, 439
Forveille, T., Guilloteau, S., & Lucas, R. 1990, IRAM internal report (CLASS)
Gavazzi, G., Pierini, D., & Boselli, A. 1996, A&A, 312, 397
Haynes, M., & Giovanelli, R. 1984, AJ, 89, 758
Karachentseva, V. 1973, Comm. Spec. Astrophys. Obs., 8
Kenney, J., & Young, J. 1989, ApJ, 344, 171
Sage, L. 1993, A&AS, 100, 537
Solomon, P., & Sage, L. 1988, ApJ, 334, 613
Strong, A., Bloemen, J., Dame, T., et al. 1988, A&A, 207, 1
Young, J., Xie, S., Tacconi, L., et al. 1995, ApJS, 98, 219
Zwicky, F., Herzog, E., Karpowicz, M., Kowal, C., & Wild, P. 1961−1968, arcsecCatalogue of Galaxies and of Cluster of Galaxies arcsec (Pasadena, California Institute of Technology; CGCG)